Sensors & Transducers, Vol. 165, Issue 2, February 2014, pp. 81-88

www.sensorsportal.com

Sensors & Transducers

http://www.sensorsportal.com

A Novel Rotor and Stator Magnetic Fields Direct-Orthogonalized Vector Control Scheme for the PMSM Servo System

Shi-Xiong Zhang
School of Mechanical & Electrical Engineering,
Henan University of Technology, No. 195, Zhongyuan Rd., Zhengzhou, 450007, P. R. China
Tel.: +86-371-67758631
E-mail: cehonzhang@gmail.com

Received: 14 November 2013 /Accepted: 28 January 2014 /Published: 28 February 2014

Abstract: Permanent Magnet Synchronous motor (PMSM) has received widespread acceptance in recent years. In this paper, a new rotor and stator Magnetic Fields Direct-Orthogonalized Vector Control (MFDOVC) scheme is proposed for PMSM servo system. This method simplified the complex calculation of traditional vector control, a part of the system resource is economized. At the same time, through the simulation illustration validation, the performance of PMSM servo system with the proposed MFDOVC scheme can achieve the same with the complex traditional vector control method, but much simpler calculation is implemented using the proposed method. *Copyright © 2014 IFSA Publishing, S. L.*

Keywords: Permanent magnet synchronous motor (PMSM), Vector control, Rotor and stator Magnetic Fields Direct-Orthogonalized Vector Control (MFDOVC), Real-time PMSM servo system.

1. Introduction

Permanent magnet synchronous motor (PMSM) has received widespread acceptance in high performance industrial servo applications of accurate speed and position control due to some of its excellent features such as super power density, high torque to current ratio, fast response and better accuracy, high frequency and low noise [1-7]. For PMSM drives, in the mid-1980s, the direct torque control (DTC) was developed to control torque and flux by directly choosing the configuration of the inverter [8]. It requires flux and torque estimators, torque and flux errors are used as inputs to hysteresis controllers and a look-up table is used to determine the appropriate configuration to minimize torque and flux errors [9]. The advantages of DTC are low dependence to machine parameters and a faster dynamic torque response [10]. However, to keep the electromagnetic torque and the flux inside hysteresis bands, a very short run-time is required for computation (generally 10 μs). Furthermore, hysteresis controllers induce a variable switching frequency which can lead to acoustic noise and is generally not suitable for electromagnetic interference issues.

The classical control technique for PMSM is the Field-oriented vector control [11, 12], this traditional vector control does not take into account the inverter switching states because the outputs of the controller are the continuous voltages applied to the motor [13]. A pulse width modulation (PWM) technique can be used to translate these voltages into the switching states of the inverter.

In this paper, a new rotor and stator Magnetic Fields Direct-Orthogonalized Vector Control (MFDOVC) scheme is proposed for PMSM servo system. This method simplified the complex calculation of traditional vector control, a part of the system resource is economized. At the same time, through the simulation illustration validation, the performance of PMSM servo system with the proposed MFDOVC scheme can achieve the same with the complex traditional vector control method but with much simpler calculation.

The major contributions of this paper include

1) A new a new rotor and stator magnetic fields direct-orthogonalized vector control scheme;

2) Calculation comparison between the traditional vector control and the proposed MFDOVC;

2) Simulation illustration of the MFDOVC scheme for the PMSM drive model;

3) Performance comparison between the traditional vector control and the proposed MFDOVC by performing the simulation experiment.

The rest of this paper is organized as follows. In Sec. 2, the mathematic model of the PMSM is introduced briefly and in Sec. 3, the new orthogonal magnets vector control scheme is presented and compared with the traditional vector control method. Simulation and tests are implemented in Sec. 4, the performances using the proposed OMVC are compared with the traditional vector control for the PMSM servo system. Conclusion is given in Sec. 5.

2. PMSM Model and Schematic Diagram of the PMSM Drive

Under the assumption that the saturation, eddy currents and hysteresis losses are negligible in a permanent magnetic (PM) synchronous motor [14], the mechanical equations and electrical equations of a PMSM in the synchronous rotating reference frame are given by

$$\frac{\mathrm{d}\theta}{\mathrm{d}t} = \omega, \quad \frac{\mathrm{d}\omega}{\mathrm{d}t} = \frac{1}{J}(T_m - T_l - B\omega), \tag{1}$$

$$\frac{\mathrm{d}i_d}{\mathrm{d}t} = \frac{1}{L_d}(V_d + \omega L_q i_q - Ri_d - \omega\psi_{qm}), \tag{2}$$

$$\frac{\mathrm{d}i_q}{\mathrm{d}t} = \frac{1}{L_q}(V_q - \omega L_d i_d - Ri_q - \omega\psi_{dm}), \tag{3}$$

where (1) represents the mechanical subsystem, and equations (2) and (3) represent the electrical subsystem. θ and ω are motor rotor angular position and speed, respectively; B is the friction coefficient; J is the moment of inertia of the rotor; T_m is the motor electromagnetic torque generated, and T_l is the load torque applied; i_d and i_q are stator currents along the d and q axes, respectively; V_d and V_q are the voltages along d and q axes, respectively; R is the stator resistance; L_d and L_q are the stator self-inductances in the d and q axes, respectively.

The PMSM is modeled by continuous state equations written in a rotor flux reference frame. For these state equations, there are a finite number of control vectors, eight switching states of the inverter. The simplified schematic diagram of the PMSM drive is composed of a permanent magnet synchronous machine and a two-level voltage inverter as shown in Fig. 1.

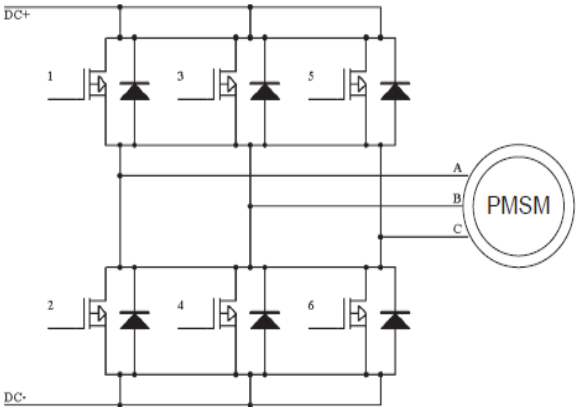

Fig. 1. A PMSM controlled by a two-level inverter.

3. Traditional Vector Control and the Rotor and Stator Magnetic Fields Direct-Orthogonalized Vector Control for the PMSM Servo System

3.1. Traditional Vector Control for PMSM Servo System

1) Speed Closed-Loop Control: Fig. 2 shows the control structure of system model with the speed and current closed loops. The speed reference is given, we can get the rotor angular information as the position feedback from the optical encoder of the PMSM module, and the derivative of the rotor angle is the speed feedback, then the speed closed-loop control can be performed. The speed and current (detailed current closed-loop control is introduced in 3.2 are both adjusted by PID control strategy. The setting of the controllers' parameters is not the focus of this paper. The following procedures are followed during the initial controller parameter setting.

• Firstly, tune the current loop to make sure that I_{dfdb} and I_{qfdb} can follow I_{dref} and I_{qref} as quickly as possible.

• Secondly, tune the speed loop to achieve the tradeoff between the response time and the overshoot of speed step response.

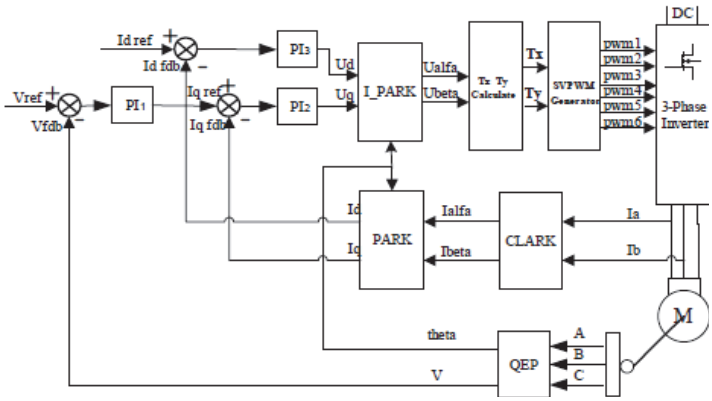

Fig. 2. Block diagram of the PMSM position servo system model.

2) Current Closed-Loop Control: In the inner current closed-loop, i_{dref} is given as 0, i_{qref} is obtained from the speed PID controller; then the stator line currents i_A and i_B are measured and the following coordinate transformations between stationary $A-B-C$ frame, stationary $\alpha-\beta$ frame and synchronously rotating $d-q$ frame [15] are performed.

• "Clark block": Stationary $A-B-C$ frame to stationary $\alpha-\beta$ frame.

$$\begin{bmatrix} i_\alpha \\ i_\beta \end{bmatrix} = \begin{bmatrix} \sqrt{\frac{3}{2}} & 0 \\ \frac{\sqrt{2}}{2} & \sqrt{2} \end{bmatrix} \begin{bmatrix} i_A \\ i_B \end{bmatrix}$$

• "Park block": Stationary $\alpha-\beta$ frame to rotating $d-q$ frame.

$$\begin{bmatrix} i_d \\ i_q \end{bmatrix} = \begin{bmatrix} \cos\theta_r & \sin\theta_r \\ -\sin\theta_r & \cos\theta_r \end{bmatrix} \begin{bmatrix} i_\alpha \\ i_\beta \end{bmatrix}$$

• "I-Park block": Rotating $d-q$ frame to stationary $\alpha-\beta$ frame.

$$\begin{bmatrix} V_\alpha \\ V_\beta \end{bmatrix} = \begin{bmatrix} \cos\theta_r & -\sin\theta_r \\ \sin\theta_r & \cos\theta_r \end{bmatrix} \begin{bmatrix} V_d \\ V_q \end{bmatrix}$$

Then the current closed-loop control can be performed, the current PID controller is introduced in III-A1. Clearly, referring to Fig. 2, the PMSM will be decoupled if the control i_d = 0 and we can control a PMSM as easily as a DC motor. The electrical and mechanical equations of PMSM are written as (1)-(3).

3) Space Vector Pulse Width Modulation (SVPWM): SVPWM is a special switching scheme of a 3-phase power converter with six power transistors. As shown in Fig. 3, the SVPWM technique is applied to approximate the reference voltage U_o, and it combines with the eights basic space vectors [15]. Therefore, the motor voltage vector U_o will be located at one of the six sectors (S1, S2, S3, S4, S5 and S6) at any given time. Thus, for any PWM period, it can be approximated by the vector sum of two vector components lying on the two adjacent basic vectors [16].

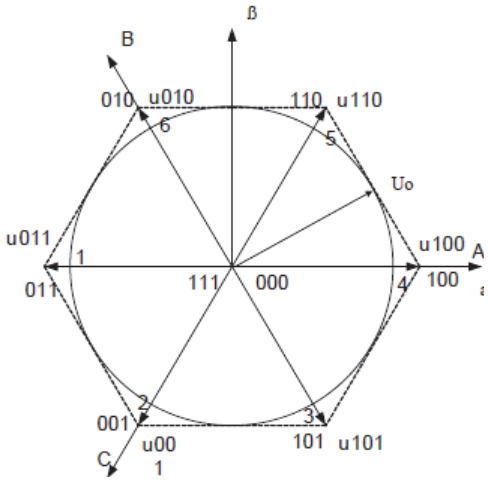

Fig. 3. Basic space vectors and switch patterns.

3.2. The Rotor and Stator Magnetic Fields Direct-Orthogonalized Vector Control (MFDOVC) for PMSM Servo System

1) The Central Principle of the MFDOVC: For the proposed MFDOVC method for PMSM drive, the key idea is that, only if the magnetic fields of the stator and rotor can be ensured to orthogonalize each other directly, then the torque of the PMSM can be controlled by modulating the currents of the stator, just like controlling a DC motor. As shown the torque equation in (4),

$$T = F_s F_r \sin\theta, \quad (4)$$

where F_s is the magnetomotive force vector of the stator, and F_r is the magnetomotive force vector of the rotor which is constant because the rotor is the permanent magnet, θ is the angle between the two magnetomotive force vectors.

In the stator frame, the space position of the vector F_r can be measured by the optical encoder of the PMSM, and the space position of the vector F_s can be calculated which will be introduced in the following sections. So, only need to keep these two magnetomotive force vectors, namely the two synthetical current vectors of the stator and rotor, orthogonal directly, that is to say $\theta = \frac{\pi}{2}$. Thus, the variables and parameters represented in the stator frame do not need to be transformed into those in the synchronous reference frame and transformed back to control the real stator currents, so the calculation is simplified and a part of the resource is saved for the PMSM servo system. For the calculation comparison with the proposed MFDOVC scheme, the previous work [16] can be referred for the traditional vector control calculation details.

As shown in Fig. 4, the three phase currents of the PMSM is synthesized into one synthetical current vector is, then the amplitude $|i_s|$ of the vector is i_s compared with the reference current vector amplitude $|i^*|$, which is calculated by the PI controller in the speed closed-loop. Referring to the tradition vector control, because the d axis reference current assigned as zero, so the q axis reference current vector stands for the synthetical reference current vector. Thus, the output of the speed closed-loop PI controller is used to be the reference current vector i^* in the proposed MFDOVC scheme.

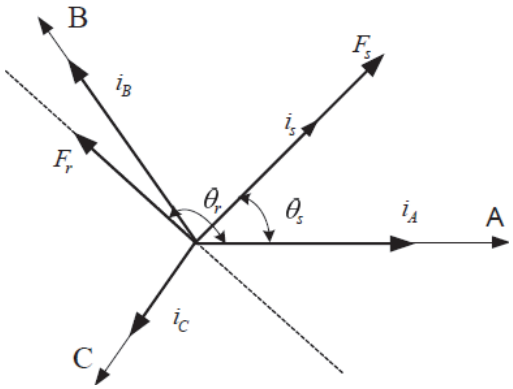

Fig. 4. The synthetical current vector for three phase current vector in the stator A-B-C reference frame.

For the realization of the PMSM drive, we also use the space vector pulse width modulation (SVPWM) scheme as in the traditional vector control. But the inputs of the parameters calculation module for the SVPWM are not the d axis and the q axis voltage output references; instead, the amplitude and the phase of the voltage output vector are calculated for the SVPWM module, the amplitude U_o as shown in Fig. 4 can be obtained from the output of the PI controller in the current closed-loop, and the phase can be calculated from another PI controller which will be introduced in section 3.2.

2) Calculation for the Amplitude of the Output Voltage Vector: in Fig. 5, it can be seen that, only two phases currents of the stator are measured, the third phase current can be calculated,

$$|i_C| = -(|i_A| + |i_B|), \tag{5}$$

so the three phase currents i_a, i_b and i_c can be fixed in the static stator A-B-C reference frame as shown in Fig. 4, and adding the three current vectors in the space,

$$\begin{aligned} i_s &= i_A + i_B + i_C \\ &= |i_A|e^{\theta_A} + |i_B|e^{\theta_B} + |i_C|e^{\theta_C}, \end{aligned} \tag{6}$$

where $|i_A|$, $|i_B|$, $|i_C|$, θ_A, θ_B and θ_C are the amplitudes and phases of the three current vectors i_A, i_B and i_C.

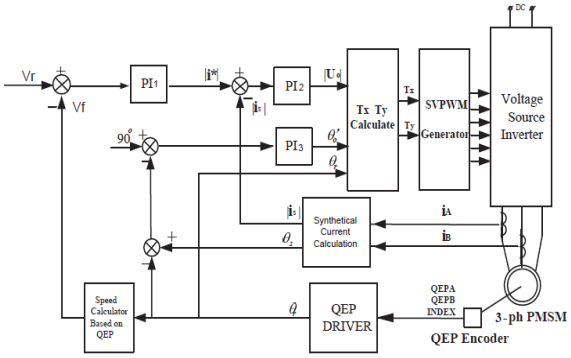

Fig. 5. The MFDOVC for PMSM Servo System.

The synthetical feedback current vector i_s can be obtained,

$$i_s = |i_s|e^{\theta_s}, \tag{7}$$

$$|i_s| = \sqrt{|i_\alpha|^2 + |i_\beta|^2}, \tag{8}$$

$$\theta_s = \arccos\left(\frac{i_\alpha}{\sqrt{i_\alpha^2 + i_\beta^2}}\right), \tag{9}$$

where $|i_s|$ and θ_s are the amplitudes and phases of the three current vectors i_s, i_α and i_β are the two current vector in static stator $\alpha - \beta$ reference frame [16].

As $\theta_A = 0^o$, $\theta_B = 120^o$ and $\theta_C = 240^o$,

$$|i_\alpha| = |i_A| - \frac{1}{2}(|i_B| + |i_C|) \tag{10}$$

$$|i_\beta| = \frac{\sqrt{3}}{2}(|i_B| - |i_C|) \tag{11}$$

Submitting (10), (11) and (5) into (8), yield,

$$|i_s| = \sqrt{|i_A|^2 + |i_A||i_B| + |i_B|^2} \tag{12}$$

$$\theta_s = \arctan(\frac{\sqrt{3}|i_A|}{|i_A| + 2|i_B|}) \tag{13}$$

The reference current vector amplitude $|i^*|$ is calculated from the PI controller in the speed closed-loop, then the voltage output vector amplitude $|U_o|$ can be obtained,

$$e_{|i|} = |i^*| - |i_s|, \tag{14}$$

$$|U_o| = K_{p2}e_{|i|} + \int_0^t K_{i2}e_{|i|}\mathrm{d}t\,, \tag{15}$$

where K_{p2} and K_{i2} are the parameters of the first PI2 controller in the current closed-loop.

3) Calculation for the Phase of the Output Voltage Vector: As shown in Fig. 5, in state stator A-B-C reference frame, the position angle θ_r of the rotor d axis can be measured by the optical encoder, and the position angle θ_s of the synthetical current vector can be calculated in (13), the position angle of the reference current i^* is $(\frac{\pi}{2} + \theta_r)$, thus the voltage output vector phase θ_o can be obtained with the saturation ±0.035 rad,

$$e_\theta = \frac{\pi}{2} + \theta_r - \theta_s\,, \tag{16}$$

$$\theta_o{}' = K_{p3}e_\theta + \int_0^t K_{i3}e_\theta\mathrm{d}t\,, \tag{17}$$

$$\theta_o = \theta_o{}' + \theta_r + \frac{\pi}{2}, \tag{18}$$

where K_{p3} and K_{i3} are the parameters of the second PI3 controller in the current closed-loop.

4) Implementation of the Space Vector Pulse Width Modulation (SVPWM): As mentioned in the tradition vector control, SVPWM is a special switching scheme of a 3-phase power converter with six power transistors, which is shown in Fig. 1. The SVPWM implementation of the proposed MFDOVC is introduced as follow:

• Step-1: Determination of the sector by lookup in the Table 1.

Table 1. Sector assignment.

θ_o	1	2	3	4	5	6
Sector	$[0,\frac{\pi}{6})$	$[\frac{\pi}{6},\frac{\pi}{3})$	$[\frac{\pi}{3},\frac{\pi}{2})$	$[\frac{\pi}{2},\frac{2\pi}{3})$	$[\frac{2\pi}{3},\frac{5\pi}{6})$	$[\frac{5\pi}{6},2\pi)$

• Step-2: Calculate the performing time T_x and T_y of the two adjacent basic voltage vector [16] U_x and U_y as show in Fig. 6,

$$|U_o|e^{\theta_o} = \frac{T_x}{T}|U_x|e^{\theta_s} + \frac{T_y}{T}|U_y|e^{\theta_y}\phi\,, \tag{19}$$

where $|U_x|$, $|U_y|$, θ_x and θ_y are the amplitudes and phases of the two basic voltage vector $|U_x|$ and $|U_y|$.

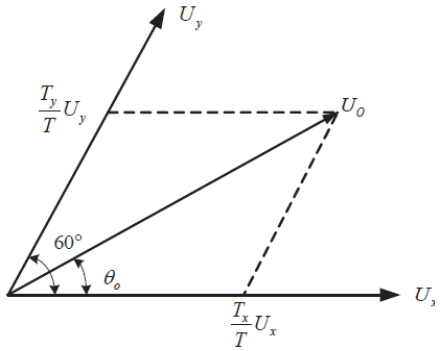

Fig. 6. The voltage space vector combination from two adjacent basic voltage vectors.

From Fig. 6, we also can get,

$$\frac{\frac{T_x}{T}|U_x|}{\sin(60^o - \theta_o)} = \frac{U_o}{\sin 120^o} \tag{20}$$

$$\frac{\frac{T_y}{T}|U_y|}{\sin\theta_o} = \frac{U_o}{\sin 120^o} \tag{21}$$

Meanwhile,

$$|U_x| = |U_y| = \sqrt{\frac{3}{2}U_D}\,, \tag{22}$$

where U_D is the generatrix voltage DC+ and DC- in Fig. 1.

Submitting (22) into (20) and (21) yield,

$$T_x = \frac{2\sqrt{2}T|U_o|\sin(60^o - \theta_o)}{3U_D}\,, \tag{23}$$

$$T_y = \frac{2\sqrt{2}|U_o|\sin\theta_o}{3U_D} \tag{24}$$

• Step-3: Determine the duty cycle T_a , T_b , T_c as follows:

$$T_{aon} = \frac{T - T_x - T_y}{2} \tag{25}$$

$$T_{bon} = T_{aon} + T_x \tag{26}$$

$$T_{con} = T_{con} + T_y \tag{27}$$

• Step-4: Assign the duty cycles T_a , T_b and T_c from Table 2, then compare with the given deltoid waveform, we can get the signals of PWM1, PWM3 and PWM5 as show in Fig. 7, and PWM2, PWM4 and PWM5 are the complementary signals of PWM1, PWM3 and PWM5 respectively. PWM1 PWM6 are used to control the power transistor switching time in the 3-Phase inverter.

Table 2. Assigning duty cycle in any sectors.

Sector	1	5	0	3	2	4
T_a	T_{aon}	T_{bon}	T_{con}	T_{con}	T_{bon}	T_{aon}
T_b	T_{bon}	T_{aon}	T_{aon}	T_{bon}	T_{con}	T_{con}
T_c	T_{con}	T_{con}	T_{bon}	T_{aon}	T_{aon}	T_{bon}

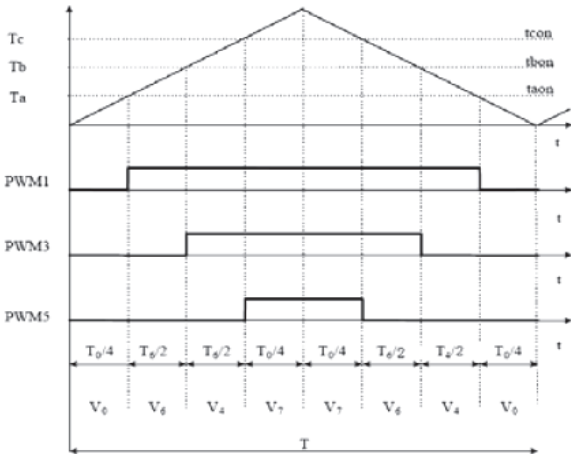

Fig. 7. PWM patterns and duty cycle [17].

4. Simulation Illustrations

In this section, we present two simulation tests to demonstrate the effectiveness of the proposed MFDOVC scheme for the PMSM speed servo control system model, Fig. 4 shows the block diagram, and compare the performance with the traditional vector control method, the block diagram of which is shown in Fig. 2.

- Case-1: Simulation unit step speed response and electromagnetic torque comparison of traditional vector control and the proposed MFDOVC schemes with idle load;
- Case-2: Simulation unit step speed response and electromagnetic torque comparison of traditional vector control and the proposed MFDOVC schemes with load $T = 2Nm$;

For comparing fairly, the parameters of the PI1, PI2 and PI3 controllers in Fig. 2 for the traditional vector control are settled as the same ones of the PI1, PI2 and PI3 controllers in Fig. 4 for the MFDOVC respectively, which have been calculated following the procedures introduced in III-A1 and correspond to $K_{p1} = 1.52$, $K_{i1} = 0.11$, $K_{p2} = 12.51$, $K_{i2} = 2.20$, $K_{p3} = 16.72$ and $K_{i3} = 1.48$. The motor parameters are given in Table 3.

Table 3. PMSM Specifications.

Rated power	1.64 kW	**Rated speed**	2000 rpm
Rated torque	8 nm	**Stator resistance**	2.125 W
Stator inductance	11.6 mH	**Magnet flux**	0.387
Number of poles	6	**Moment of inertia**	0.00289 kgm^2
Friction coefficient	0.0003 Nms		

A. Case-1: Simulation unit step speed response and electromagnetic torque comparison of the traditional vector control and the proposed MFDOVC schemes with idle load.

For this case simulation test, the following unit step velocity reference signal and load torque are used:

$$\omega_r = 500rpm, \;\; T_l = 0Nm \,,$$

Fig. 8 and Fig. 10 show the unit step speed responses of traditional vector control and the proposed MFDOVC schemes with idle load, we can see, the MFDOVC method performs as well as the traditional vector control method for the speed response. Meanwhile, the effectiveness of the MFDOVC also can be seen through the comparison of Fig. 9 and Fig. 11, which present the electromagnetic torque output of the unit step speed response in Fig. 8 and Fig. 10.

B. Case-2: Simulation unit step speed response and electromagnetic torque comparison of the traditional vector control and the proposed MFDOVC schemes with load *T=2Nm*.

In this case, the following unit step velocity reference signal and load torque are used:

$$\omega_r = 500rpm, \;\; T_l = 2Nm$$

Fig. 12 - Fig. 15 show the unit step speed responses and electromagnetic torque comparison of traditional vector control and the proposed MFDOVC schemes with *T=2Nm* load, it also can be seen that, the MFDOVC method performs as well as the traditional vector control method.

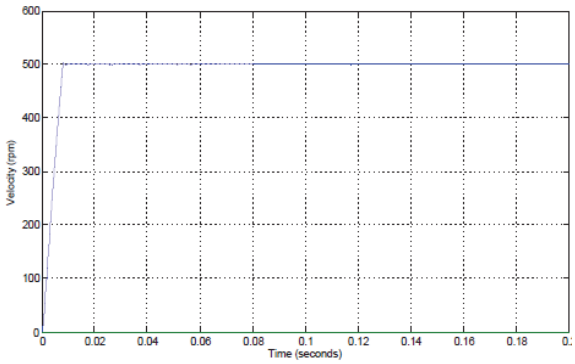

Fig. 8. Simulation. Unit step speed response of the traditional vector control for the PMSM servo system with idle load.

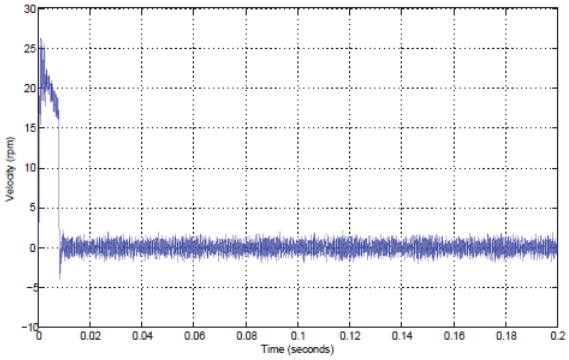

Fig. 9. Simulation. Electromagnetic torque output of the unit step speed response in Fig. 9 with idle load.

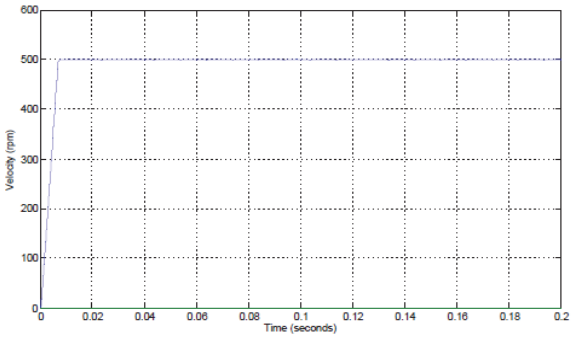

Fig. 10. Simulation. Unit step speed response of the proposed MFDOVC for the PMSM servo system with idle load.

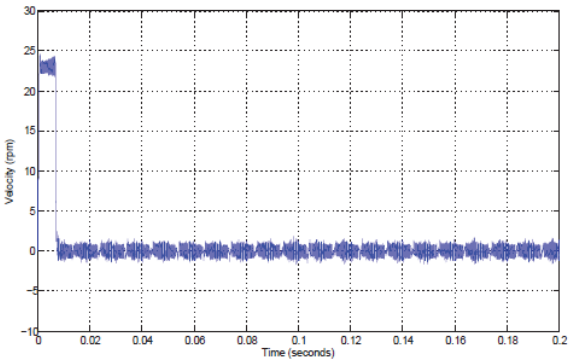

Fig. 11. Simulation. Electromagnetic torque output of the unit step speed response in Fig. 11 with idle load.

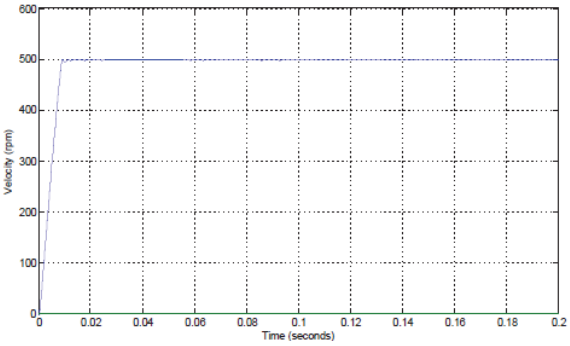

Fig. 12. Simulation. Unit step speed response of the traditional vector control.

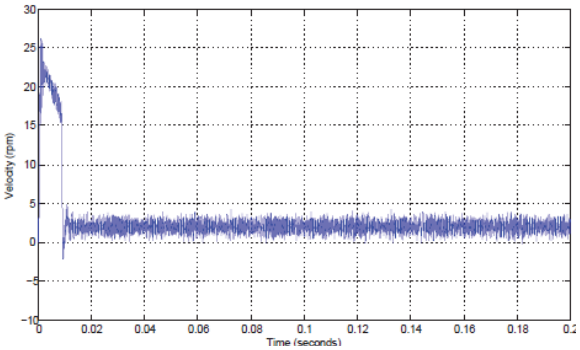

Fig. 13. Simulation. Electromagnetic torque output of the unit step speed response in Fig. 13 with load T = 2Nm.

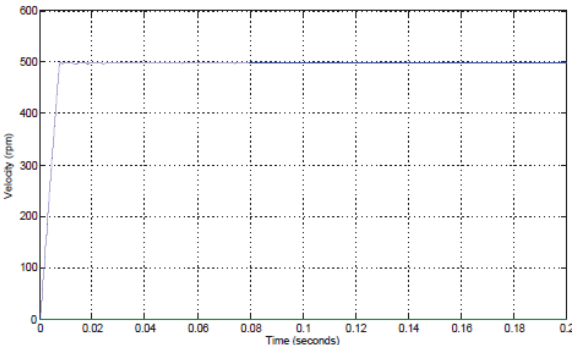

Fig. 14. Simulation. Unit step speed response of the proposed MFDOVC for the PMSM servo system with load T = 2Nm.

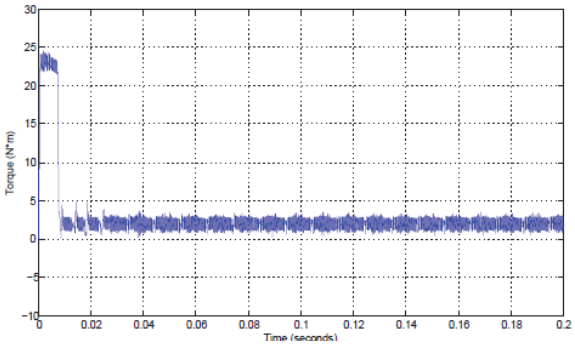

Fig. 15. Simulation. Electromagnetic torque output of the unit step speed response in Fig. 15 with load T = 2Nm.

Most important, comparing with the traditional vector control method, the proposed MFDOVC strategy simplified the calculation, it is easier to realize in the real-time PMSM servo drive system.

5. Conclusions

In this paper, a new stator and rotor magnetic fields direct-orthogonalized vector control scheme for the PMSM servo control system. In the MFDOVC, only need to orthogonalize the two magnetomotive force vectors of the stator and rotor directly, then the variables and parameters represented in the stator frame do not need to be transformed into those in the synchronous reference frame and transformed back to control the real stator currents, so the calculation is simplified and a part of the resource is saved for the PMSM servo system. From the simulation and experimental results, we can conclude that, the proposed MFDOVC method performs as well as the traditional vector control method. In particularly, comparing with the traditional vector control method, the proposed MFDOVC strategy simplified the calculation, it is easier to realize in the real-time PMSM servo drive system.

Acknowledgements

The author wishes to acknowledge the supports by the Natural Science Fund of Henan Education Department (Project ID:13A460189), the Natural Science Fund of Henan Science & Technology Depart (Project ID:132102110255), and the Science Foundation of Henan University of Technology (Project ID:2010BS049).

References

[1]. P. Pillay, R. Krishnan, Control characteristics and speed controller design of a high performance PMSM, in *Proceeding of the IEEE Industrial Application. Soc. Annual. Meetin. Rec.,* 1985, pp. 627-633.

[2]. M. A. Rahman, M. A. Hoque, On-line adaptive artificial neural network based vector control of permanent magnet synchronous motor, *IEEE Transaction on Energy Conversion.*, 13, 4, 1998, pp. 311-318.

[3]. Y. Zhang, C. M. Akujuobi, W. H. Ali, C. L. Tolliver, L.-S. Shieh, Load disturbance resistance speed controller design for PMSM, *IEEE Transaction on Industrial Electron.*, 53, 4, 2006, pp. 1198-1208.

[4]. M. N. Uddin, M. A. Rahman, High-speed control of IPMSM drives using improved fuzzy logic algorithms, *IEEE Transaction on Industrial Electron.*, 54, 1, 2007, pp. 190-199.

[5]. C. Cecati, M. Tursini, Vector control algorithms implementation for inverter-fed permanent magnet synchronous motor using transputer, in *Industrial Electronics Control and Instrumentation Proceedings on (IECON'91)*, Oct. 1991, pp. 171-176.

[6]. Shigeo Morimoto, Keita Hantanaka, Wide-speed operation of interior permanent magnet synchronous motors with high-performance current regulator, *IEEE Transaction on Industrial Application*, 30, 4, 1994, pp. 920-926.

[7]. Jun Zhang, Xu Wang, PMSM vector control and initial magnetic pole position detect method based on DSP, in *Intelligent Control and Automation (WCICA)*, June 2006, pp. 8265-8269.

[8]. I. Takahashi, T. Noguchi, A new quick-response and high efficiency control strategy of an induction motor, *IEEE Transaction on Industrial Application*, IA-22, 5, 1986, pp. 820-827.

[9]. P. Vas, Sensorless Vector and Direct Torque Control, *Oxford University Press*, 1998.

[10]. G. S. Buja, M. P. Kazmierkowski, Direct torque control of PWM inverter-fed AC motors - a survey, *IEEE Transaction on Industrial Electron*, 51, 4, 2004, pp. 744-757.

[11]. F. Blaschke, The principle of field orientation as applied to the new transvector closed-loop control system for rotating field machines, *Siemens Review*, 39, 3, 1972, pp. 217-220.

[12]. Karl-Heinz Bayer, Hermann Waldmann, Field-oriented closed loop control of a synchronous machine with the new transvertor control system, *Siemens Review*, 39, 3, 1972, pp. 217-220.

[13]. W. Leonhard, Control of Electrical Drives, 2nd ed., *Springer-Verlag*, Berlin, 1990.

[14]. P. C. Krause, Analysis of electric machinery, *McGraw-Hill*, New York, 1987.

[15]. B. K. Bose, Power electronics and variable frequency drives - technology and application, *IEEE Press*, 1997.

[16]. Ying Luo, Yang Quan Chen, You Guo Pi, Authentic simulation studies of periodic adaptive learning compensation of cogging effect in PMSM position servo system, in *Proceeding of the Chinese Conference on Decision and Control 2008 (CCDC'08)*, Yantai, Shandong, China, 2008.

[17]. Ying-Shieh Kung, Pin-Ging Huang, High performance position controller for PMSM drives based on TMS320F2812 DSP, in *Proceedings of the IEEE International Conference*, Sept. 2004, pp. 290-295.